Volume 1 | Number 1 | Jan 2013 | Pages 1–100

Analytical Methods

www.rsc.org/methods

ROYAL SOCIETY OF CHEMISTRY

This is an *Accepted Manuscript*, which has been through the Royal Society of Chemistry peer review process and has been accepted for publication.

Accepted Manuscripts are published online shortly after acceptance, before technical editing, formatting and proof reading. Using this free service, authors can make their results available to the community, in citable form, before we publish the edited article. We will replace this *Accepted Manuscript* with the edited and formatted *Advance Article* as soon as it is available.

You can find more information about *Accepted Manuscripts* in the **Information for Authors**.

Please note that technical editing may introduce minor changes to the text and/or graphics, which may alter content. The journal's standard **Terms & Conditions** and the **Ethical guidelines** still apply. In no event shall the Royal Society of Chemistry be held responsible for any errors or omissions in this *Accepted Manuscript* or any consequences arising from the use of any information it contains.

www.rsc.org/methods

Label-free and real-time monitoring of trypsin activity in living cells by quantum-dot-based fluorescent sensors

Wenzhu Zhang,[a] Ping Zhang,[a] Shengzhou Zhang*[b] and Changqing Zhu*[a]

[a] *Anhui Key Laboratory of Chemo-Biosensing, College of Chemistry and Materials Science, Anhui Normal University, Wuhu, 241000, P. R. China. E-mail: zhucq@mail.ahnu.edu.cn*

[b] *Anhui Key Laboratory of Biotic Environment and Ecological safety, College of Life Science, Anhui Normal University, Wuhu, 241000, P. R. China. E-mail: szzhang@mail.ahnu.edu.cn*

Abstract: In this study, a quantum dots (QDs)-based label-free fluorescence assay has been developed for real-time monitoring of intracellular trypsin activity and screening the corresponding inhibitor. Negatively charged CdTe QDs and positively charged cytochrome c (cyt.c) first form a hybrid complex structure through electrostatic attraction effect. The fluorescence of the QDs is well quenched because of electron transfer from QDs to cyt.c. Then, added trypsin breaks the hybrid complex structure because of the hydrolysis of cyt.c catalyzed by the trypsin. Thus, the electron transfer is switched off and a substantial fluorescence recovery is obtained. Under optimal conditions, the initial rate of the hydrolysis reaction is linearly proportional to the concentration of trypsin between 1.25 and 375 nM, and the detection limit is as low as 0.42 nM. The proposed method is effective, simple and cost-effective, demonstrating the great potential for point-of-care diagnosis applications.

Keywords: trypsin activity; label-free fluorescent assay; quantum dots; cell imaging

1. Introduction

Trypsin is one of the most important digestive enzymes produced by the pancreas, and it plays a key role in controlling the pancreatic exocrine function.[1] Trypsin is involved in the digestive enzyme activation cascade, which induces the transformation of other pancreatic proenzymes into their active forms within the intestine and then initiates autodigestion.[2] Some diseases are correlated to the change of the trypsin level, such as cystic fibrosis,[3] pancreatic carcinoma,[4] pancreatitis,[5] necrosis,[6] meconium ileus[7] and apoptosis.[8] Therefore, simple and effective assay for

trypsin activity monitoring and corresponding inhibitor screening may lead to new diagnostic methods and even unprecedented therapeutic implications for these diseases.

Hitherto, a number of methods have been reported for trypsin activity study, including enzyme-linked immunosorbent assay,[9] gelatin-based film technique,[10] electrochemistry[11] and fluorescence spectroscopy. Among them, fluorescence technique offers significant advantages because of high sensitivity, simplicity, and nondestruction. Moreover, fluorescence microscopic imaging allows us to map the spatial and temporal distribution of trypsin. To date, a variety of fluorescent assays have been designed for trypsin sensing. For example, Josephson's group performed a trypsin assay by using near-infrared fluorescence dyes attached to polyarginyl peptides.[12,13] Zhang et al constructed a fluorescein-labeled peptide composed of six arginine residues and graphene oxide for trypsin assay and inhibitor screening.[14] Tang and co-workers developed a trypsin assay based on a fluorescein-labeled functionalized fullerene derivative;[15] then, they further constructed a self-assembly nanoprobe, mercaptoethylamine-modified-gold nanoparticles-lysine-bridged-bis (β-cyclodextrins)-fluorescein, which was successfully applied to the determination of trypsin in biological systems.[16] However, most of the existed probes involve in complicated synthesis processes, and that fluorescence label technique is often necessary for an efficient signal response.

Compared with fluorescence labeling technique, label-free strategy not only reduce the cost, but provide assay accuracy because covalent conjugation of labeling processes often impair the catalytic turnover of the enzymes.[17,18] Therefore, label-free assays for trypsin have been developed recently. For example, Tang's[19] and Zhang's[20] group independently reported label-free fluorescence methods based on the aggregation-induced emission of tetraphenylethene. Meanwhile, Liu and co-workers designed a water-soluble carboxylated polyfluorene derivative (PFP-CO$_2$Na) for monitoring trypsin activity [21] However, whether label-free fluorescent assays can achieve trypsin activity assay in complex bio-systems, such as at cell level, has remained an open question.

Herein, we have presented a quantum dots (QDs)-based label-free fluorescence assay for real-time monitoring of intracellular trypsin activity and screening the corresponding inhibitor. The sensing principle is shown in Scheme 1: negatively charged CdTe QDs and positively charged cyt.c first form a hybrid complex structure through electrostatic attraction effect. The fluorescence

of the QDs is well quenched because of electron transfer from QDs to cyt.c.[22] Then, added trypsin breaks the hybrid complex structure because trypsin catalyzes the hydrolysis of peptide bonds by the C side of lysine or arginine in cyt.c to negatively charged heme-containing fragments.[23,24] Thus, the electron transfer is switched off due to electrostatic repulsion between the QDs and fragments and a substantial fluorescence recovery is obtained. Under optimal conditions, the initial rate of the hydrolysis reaction is linearly proportional to the concentration of trypsin between 1.25 and 375 nM, and the detection limit is as low as 0.42 nM. The proposed method is effective, simple and cost-effective, demonstrating the great potential for point-of-care diagnosis applications.

Scheme 1

2. Experimental section

2.1 Materials

Te powder (60 mesh, 99.999%) was purchased from Alfa Aesar Corporation. Cytochrome c was purchased from Aladdin Corporation. The trypsin from porcine pancreas and alkaline phosphatase (ALP) were purchased from Biodee Biotechnology Co. Ltd. (Beijing). The reduced glutathione (GSH), glucose oxidase, pepsin, lipase, α-amylase, bovine serum albumin (BSA) and the BBI inhibitor [trypsin inhibitor from soybean, Bowman–Birk type] were ordered from Sangon Biotech Co. Ltd (Shanghai). Lysozyme was from J&K chemical. Thrombin was purchased from Hualanchem Co. Ltd (Shanghai). $NaBH_4$, $CdCl_2 \cdot 2.5H_2O$, trihydroxymethyl aminomethane (Tris), HCl, NaOH and other routine chemicals were acquired from Shanghai Reagent Co. All solutions were prepared with double deionized water (DDW).

2.2 Instruments

A Hitachi-U-3010 spectrometer was used to record the UV−vis absorption spectra. Steady-state fluorescence measurements were performed using a Hitachi F-4500 spectrofluorometer equipped with a R3896 red-sensitive multiplier and a 1 cm quartz cuvette. Characterizations of transmission electron microscopy (TEM) were carried out on Tecnai G2 20 ST (FEI) under the accelerating voltage of 200 kV. The image of cells was taken on the inverted fluorescence microscope

(Olympvs ckx41). All pH values were measured with a model pHs-3c pH meter.

2.3 Preparation and purification of GSH-CdTe QDs

GSH-CdTe QDs were synthesized in aqueous solution based on previously described methods with minor modifications.[22,25] Briefly, fresh NaHTe aqueous solution, which was prepared by reaction of 8.0 mg Te powder and 5.0 mg $NaBH_4$ in 0.2 mL water at 0–4 ℃ for 8 h, was injected into 100 mL oxygen-free aqueous solution containing 192 mg reduced glutathione and 57 mg of $CdCl_2 \cdot 2.5H_2O$ at pH 11.0. Then the mixture solution was heated and further refluxed in an oil bath. The reflux was stopped when the emission maximum of GSH-CdTe QDs reached 656 nm with an excitation of 380 nm. The obtained GSH-CdTe QDs were mixed with acetone, and separated by centrifugation. The precipitate was collected, and then was dried overnight under vacuum at 40 ℃. Then, the dried GSH-CdTe QDs were redissolved in 100 mL of DDW for stock solution and the concentration of GSH-CdTe QDs was estimated to be 5.34 μM.[26]

2.4 Trypsin activity assay

Different concentrations of trypsin (0 to 375 nM) were added into the solution of QDs (53.4 nM) and cyt.c (140 nM) in a Tris-HCl buffer (50 mM, pH = 8.5). After incubation at 37 ℃, the solution fluorescence spectra were measured at 60 s intervals.

2.5 The inhibition effect of BBI

Trypsin (125 nM) and different concentrations of BBI (0 to 0.4 μg mL^{-1}) were preincubated at room temperature for 15 min. The mixtures were added into the solution of QDs (53.4 nM) and cyt.c (140 nM) in 50 mM Tris-HCl buffer (pH = 8.5). After incubation at 37 ℃, the solution fluorescence spectra were measured at 60 s intervals.

2.6 Trypsin detection in serum

The normal adult human serum and acute pancreatitis adult human serum samples were obtained by centrifuging (1000 rpm, 5 min) the fresh blood samples respectively (provided by Yijishan Hospital of Wannan Medical College in Wuhu, Anhui province of China). In a typical test, Tris-HCl buffer (50 mM, pH = 8.5) and cyt.c (140 nM) were added to 1 mL volumetric bottle with

QDs (53.4 nM). Then, different amounts of serum samples or trypsin were placed in the volumetric bottle. The mixture was diluted to 1 mL with DDW and incubated at 37 ℃. Serum was treated with BBI for 15 min before reaction with hybrid QDs-cyt.c complex in control experiment.

2.7 Cell culture

Human pancreatic carcinoma (PANC-1) cells were grown in cell culture media and incubated at 37 ℃ in a humidified incubator with 5% CO_2. The cell culture medium was high glucose Dulbecco's Modified Eagle Medium (DMEM, 4.5 g glucose L^{-1}) supplemented with 10% fetal bovine serum, $NaHCO_3$ (2.0 g L^{-1}) and 1% antibiotics (penicillin/streptomycin, 100 U mL^{-1}). Cells were subcultured for 24 h before experiments to produce a concentration just below confluence.

3. Results and discussion

3.1 Characterization of the GSH-CdTe QDs.

As shown in Fig. 1A, the absorption and the emission peaks are at 584 nm and 656 nm, respectively. Bright red fluorescence of the QDs can be clearly observed under ultraviolet (UV) light (inset of Fig. 1A). The TEM image (Fig. 1B) shows that the QDs possessed a good crystalline structure with diameter about 4 nm. Particularly, the as-prepared QDs solution was stable for more than 6 months without notable precipitation in dark conditions. It should be noted that the emission band of the QDs located at near-infrared range (650-900 nm), which can improve tissue penetration, lower background interference, and reduce photochemical damage.[27-29] In this experiment a maximum emission of 656 nm was chosen. Further increasing emission wavelength would reduce the emission efficiency and stability of QDs according to our observation.

Fig. 1

3.2 Optimization of experimental conditions

The pH effects were firstly studied because of two reasons. Firstly, pH value could profoundly affect the fluorescence of CdTe QDs.[30-32] Concerning the bio-sensing applications, we investigated

the pH effects on the trypsin assay in the range of 6.5-9.5. As described in Fig. S1 (see Supporting Information), the fluorescence of the QDs increased with the enhancement of pH in the range of 6.5-9.5. So, a base condition is desirable for a bright fluorescence, especially for considering the employment for cell imaging. Then, the isoelectric point of cyt.c is 10.83, and the isoelectric point of metal-containing heme peptide fragment (electron acceptor site of cyt.c) is about 7.0; on the other hand, the isoelectric point of QDs stabilizer (GSH) is 5.93. So, the used pH value should be in the range of 7.0-10.8 for an efficient fluorescent quenching by the formation of hybrid QD-cyt.c complex and subsequent fluorescent recovery by trypsin catalysis effect based on electrostatic attraction and repulsion, respectively. As described in Fig. 2, both quenching and recovery efficiencies[33] can reach to their maximum values in the pH of 8.5-9.0. As considering above two aspects, the pH was set at 8.5 in the experiments.

Fig. 2

The concentration of used cyt.c was then studied. Higher concentration of cyt.c would cause a decrease of fluorescence responses because of the impact of free cyt.c. In contrast, too low concentration led to a higher background because the fluorescence of the QDs could not be well quenched. Obviously, both of the two cases could cause the decrease of the assay sensitivity. Our study indicated that 140 nM of cyt.c was appropriate for the assay.

3.3 Trypsin assay and analytical performances

As shown in Fig. 3A, the fluorescence was significantly quenched with addition of 140 nM cyt.c to the solution of QDs. Then the fluorescence of the QDs-cyt.c returned gradually with the increase of added trypsin, and the fluorescence intensity can recovered to 85% of the original QDs in the presence of 375 nM trypsin. Impressively, the linear range of the proposed method span more than two orders of magnitude (1.25-375 nM), and the detection limit is as low as 0.42 nM, which will be discussed in detail later.

Fig. 3

To evaluate the selectivity of the proposed method, the effects of some coexisting species in biological systems, especially in serum, on the fluorescence of QDs-cyt.c complex were studied. As described in Fig. 3B, most of the potential interfering substances (including ALP, lysozyme, thrombin, glucose oxidase, pepsin, lipase, α-amylase, BSA, proline, glycine, tyrosine, cysteine, glutamic acid, aspartic acid and methionine) cannot cause an observable fluorescence recovery of QDs-cyt.c complex. This result demonstrates that the proposed method possess high selectivity for trypsin, indicating its applicability for bio-samples. Obviously, the intense interaction of cyt.c with the glutathione on the surface of QDs, and the hydrolysis of cyt.c specifically catalyzed by the trypsin should account for the above good analytical performance.

3.4 Determination of trypsin-catalyzed cyt.c hydrolysis kinetic parameters

To examine whether the QDs-cyt.c complex could be used for real-time trypsin activity investigation, the trypsin-catalyzed hydrolysis of cyt.c as a function of time at different enzyme concentrations was plotted. Fig. 4A shows plots of the fluorescence intensity at 656 nm versus the reaction time for the QDs-cyt.c with different amounts of trypsin. The fluorescence intensities increased after the addition of trypsin. Moreover, the higher the amount of trypsin in the solution, the more quickly the fluorescence intensity of the QDs-cyt.c increased, which could be further demonstrated by the initial rate (v_0) of trypsin-catalyzed reaction.

The concentration of cyt.c during the assay, $[cyt.c]_t$ was calculated from the time-varying fluorescence intensity in Fig. 4A,[34] which as a function of time was shown in Fig. S2. The slopes of the plots at early time were calculated to afford values of v_0 for the different amounts of trypsin. As shown in Fig. 4B, v_0 was directly proportional to concentration of trypsin in the range of 1.25–375 nM, which indicated that the reaction was kinetically controlled by trypsin. The analytical detection limit was as low as 0.42 nM (10 ng mL^{-1}), which was lower than that of some fluorescence assays reported recently.[14,16,21] Impressively, these results clearly manifested that the present method was very time-saving and trypsin activity can be well evaluated within one minute even its concentration is low to nanomole level.

Kinetic study was carried out via Michaelis-Menten analysis to further demonstrate the feasibility of the real-time trypsin activity assay.[34] Fig. S3 illustrated the natural logarithm of $[cyt.c]_t$ as a function of the incubation time. The slopes of the plots at early time were computed to

afford values of V_{max}/K_m at different trypsin concentrations (V_{max} is the maximum rate of the enzyme-catalyzed reaction at the saturation substrate concentration; K_m is the Michaelis-Menten constant, which is the substrate concentration where the rate of the enzyme-catalyzed reaction is half V_{max}). As shown in Fig. 4C, V_{max}/K_m was directly proportional to the concentration of trypsin, and the slope of this linear plot afforded a value for the specificity constant (k_{cat}/K_m, k_{cat} is the catalytic constant or turnover number), $k_{cat}/K_m = 6150$ M^{-1} s^{-1}, which was in good agreement with values obtained using other assays.[21,35-37] These results demonstrated that it was possible to monitor trypsin in real time and calculate enzyme kinetic parameters on the basis of the fluorescence change of the QDs-cyt.c complex.

Fig. 4

3.5 Inhibition of trypsin catalysis

It is well known that the enzymatic activity can be inhibited by corresponding inhibitors. The hydrolysis of cyt.c catalyzed by trypsin will be retarded in the presence of the corresponding inhibitors of trypsin. Accordingly, less fluorescence increase for the QDs-cyt.c complex containing trypsin is expected after further addition of the inhibitors. Fig. 5A shows the real-time fluorescence intensity change of the QDs-cyt.c in the presence of trypsin and different amounts of BBI. The fluorescence recovery of QDs decreased with the increase of BBI amount, indicating that the overall inhibition is more effective at high inhibitor concentrations. The slopes of the plots at early time in Fig. 5A were computed to afford values of the initial rate of trypsin-catalyzed hydrolysis reaction v_0' at different BBI concentrations. As shown in Fig. 5B, the v_0' and BBI amount exhibited a good linear relationship, and the higher inhibitor concentration led to lower v_0' values. The result illustrated that the QDs-cyt.c complex could be employed for screening trypsin inhibitors. Moreover, based on the plot of the inhibition efficiency[38] versus the concentration of BBI (Fig. 5C), the corresponding IC$_{50}$ value (the concentration of the inhibitor that leads to 50% inhibition of the enzyme activity) of BBI toward trypsin was estimated to be 0.24 μg mL^{-1}. This IC$_{50}$ value of BBI was lower than that previously reported,[14] which indicated that this new method with the QDs-cyt.c complex was sensitive for screening trypsin inhibitors.

Fig. 5

3.6 Analytical applications

3.6.1 Determination of trypsin in human serum

As we known, the trypsin level would be increased[39] if people suffer from some types of pancreatic diseases. To assess the practical applicability, the proposed method was applied to analysis of trypsin level in both normal and acute pancreatitis adult human serum. As described in Tables 1 and 2 the measured trypsin level of acute pancreatitis is higher than that of normal one, and both of them are good in agreement with the reports of literature.[40] The recoveries were in the range of 97.8%–103.3% with less than 5% RSD, indicating that the present method was feasible and reliable. Furthermore, the activity of trypsin obviously decreased (Table 2) with the addition of BBI, which further demonstrated the QDs-cyt.c complex had high specificity for trypsin.

Table 1

Table 2

3.6.2 Cell imaging

Finally, the present method was applied to monitoring trypsin activity in living PANC-1 cells. We chose low concentration of the QDs (53.4 nM) with short incubation time (30 min) for avoiding potential QDs cytotoxicity,[41] although GSH-capped QDs are rather biocompatible.[42-46] As shown in Fig. 6A, intense red fluorescence can be distinctly observed at cytosol after 30 min incubation. Interestingly, the fluorescence obviously decreased as the cells were pretreated with BBI for 15 min, and that the decrease degree was closely related to the amounts of added BBI (Fig. 6B, 6C). These results indicated that the proposed label-free method can well monitor both trypsin activity and BBI inhibition effects at cell level. Especially, the bright-field images (Fig. 6D, 6E, 6F) showed the clear contour of the cells, which indicated that they were adherent cells and viable throughout the imaging experiments.[47] So, the present QDs-cyt.c based assay is promising for diagnostic methods of pancreatic diseases.

Fig. 6

9

4. Conclusions

In summary, a new method was designed to realize real-time monitoring the activity of trypsin and screening the trypsin inhibitor. It has been successfully used for the sensing of trypsin in living cells and human serum samples. The simple method with facile QDs and label-free strategy makes the routine assay of trypsin activity easier to be realized, showing great promise for the development of efficient diagnostic and therapeutic methods toward some pancreatic diseases. Meanwhile, the new fluorescence turn-on design may be extended to other luminescent materials (such as biocompatible carbon quantum dots) and protein substrates for various enzyme activity studies in a similar fashion.

Acknowledgments

Appendix A. Supplementary materials

Supplementary materials associated with this article can be found in the online version at

doi:10.1016/j.bios.2013.03020.

References

1 M. Hirota, M. Ohmuraya and H. Baba, *J. Gastroenterol.*, 2006, 41, 832-836.

2 W. X. Xue, G. X. Zhang and D. Q. Zhang, *Analyst*, 2011, 136, 3136-3141.

3 A. F. Heeley and D. G. Fagan, *Lancet*, 1984, 323, 169-170.

4 O. H. Kang, H. J. Jeong, D. K. Kim, S. C. Choi, T. H. Kim, Y. H. Nah, H. M. Kim and Y. M. Lee, *Cell Biochem. Funct.*, 2003, 21, 161-167.

5 R. J. Klaveren, P. H. M. Mulder, A. M. T. Boerbooms, C. A. Kaa, U. J. G. M. Haelst, D. J. T. Wagener and J. C. M. Hafkenscheid, *Gut*, 1990, 31, 953-955.

6 P. G. Noone, Z. Q. Zhou, L. M. Silverman, P. S. Jowell, M. R. Knowles and J. A. Cohn, *Gastroenterology*, 2001, 121, 1310-1319.

7 K. Ochiai, K. Kaneko, M. Kitagawa, H. Ando and T. Hayakawa, *Dig. Dis. Sci.*, 2004, 49, 1953-1956.

8 M. Seiberg, S. Wisniewski, G. Cauwenbergh and S. S. Shapiro, *Dev. Dyn.*, 1997, 208, 553-564.

9 M. B. Rhodes, R. M. Hill and R. E. Feeney, *Anal. Chem.*, 1957, 29, 376-378.

10 A. D. Kersey, T. A. Berkoff and W. W. Morey, *Opt. Lett.*, 1993, 18, 1370-1372.

11 R. E. Ionescu, S. Cosnier and R.S. Marks, *Anal. Chem.*, 2006, 78, 6327-6331.

12 L. Josephson, M. F. Kircher, U. Mahmood, Y. Tang and R. Weissleder, *Bioconjugate Chem.*, 2002, 13, 554-560.

13 M. F. Kircher, R. Weissleder and L. Josephson, *Bioconjugate Chem.*, 2004, 15, 242-248.

14 X. G. Gu, G. Yang, G. X. Zhang, D. Q. Zhang and D. B. Zhu, *Appl. Mater. Interfaces*, 2011, 3, 1175-1179.

15 K. H. Xu, F. Liu, J. Ma and B. Tang, *Analyst*, 2011, 136, 1199-1203.

16 P. Li, Y. Liu, X. Wang and B. Tang, *Analyst*, 2011, 136, 4520-4525.

17 P. J. Hergenrother, M. R. Spaller, M. K. Haas and S. F. Martin, *Anal. Biochem.*, 1995, 229, 313-316.

18 S. Kurioka and M. Matsuda, *Anal. Biochem.*, 1976, 75, 281-289.

19 J. P. Xu, Y. Fang, Z. G. Song, J. Mei, L. Jia, A. J. Qin, J. Z. Sun, J. Ji and B. Z. Tang, *Analyst*, 2011, 136, 2315-2321.

20 W. G. Xue, G. X. Zhang, D. Q. Zhang and D. B. Zhu, *Org. Lett.*, 2010, 12, 2274-2277.

21 Y. Y. Wang, Y. Zhang and B. Liu, *Anal. Chem.*, 2010, 82, 8604-8610.

22 M. Cao, C. Cao, M. G. Liu, P. Wang and C. Q. Zhu, *Microchim. Acta*, 2009, 165, 341-346.

23 J. M. Busnel, S. Descroix, T. Le Saux, S. Terabe, M. C. Hennion and G. Peltre, *Electrophoresis*, 2006, 27, 1481-1488.

24 T. Zhang, H. L. Fan, J. G. Zhou, G. L. Liu, G. D. Feng and Q. H. Jin, *Macromolecules*, 2006, 39, 7839-7843.

25 Y. S. Xia, L. Song and C. Q. Zhu, *Anal. Chem.*, 2011, 83, 1401-1407.

26 W. W. Yu, L. H. Qu, W. Z. Guo and X. G. Peng, *Chem. Mater.*, 2003, 15, 2854-2860.

27 D. H. Hu, P. F. Zhang, P. Gong, S. H. Lian, Y. Y. Lu, D. Y. Gao and L. T. Cai, *Nanoscale*, 2011, 3, 4724-4732.

28 G. X. Liang, L. L. Li, H. Y. Liu, J. R. Zhang, C. Burda and J. J. Zhu, *Chem. Commun.*, 2010, 46,

2974-2976.

29 Q. Ma and X. G. Su, *Analyst*, 2010, 135, 1867-1877.

30 J. Chen, Y. C. Gao, Z. B. Xua, G. H. Wu, Y. C. Chen and C. Q. Zhu, *Anal. Chim. Acta*, 2006, 577, 77-84.

31 L. Shang, L. H. Zhang and S. J. Dong, *Analyst*, 2009, 134, 107-113.

32 Y. S. Xia and C. Q. Zhu, *Microchim. Acta*, 2009, 164, 29-34.

33 B. Y. Han, J. P. Yuan and E. K. Wang, *Anal. Chem.*, 2009, 81, 5569-5573.

34 Y. Liu, K. Ogawa and K. S. Schanze, *Anal. Chem.*, 2008, 80, 150-158.

35 R. M. Caprioli and L. Smith, *Anal. Chem.*, 1986, 58, 1080-1083.

36 G. J. Huang, Y. L. Ho, H. J. Chen, Y. S. Chang, S. S. Huang, H. J. Hung and Y. H. Lin, *Bot. Stud.*, 2008, 49, 101-108.

37 K. Kang, C. Y. Kan, A. Yeung and D. S. Liu, *Macromol. Biosci.*, 2005, 5, 344-351.

38 V. M. Ho and T. B. Ng, *J. Pept. Sci.*, 2008, 14, 278-282.

39 P. G. Lankisch, S. Burchard-Reckert and D. Lehnick, *Gut*, 1999, 44, 542-544.

40 J. M. Artigas, M. E. Garcia, M. R. Faure, A. M. Gimeno, *Postgrad. Med. J.*, 1981, 57, 219-222.

41 H. F. Qian, C. Q. Dong, J. F. Weng and J. C. Ren, *Small*, 2006, 2, 747-751.

42 M. Xue, X. Wang, H. Wang and B. Tang, *Talanta*, 2011, 83, 1680-1686.

43 A. M. Derfus, W. C. W. Chan, S. N. Bhatia, *Nano Lett.*, 2004, 4, 11-18.

44 W. B. Chen, X. J. Tu and X. Q. Guo, *Chem. Commun.*, 2009, 1736-1738.

45 C. Zhou, M. Long, Y. P. Qin, X. K. Sun and J. Zheng, *Angew. Chem. Int. Ed.*, 2011, 50, 3168-3172

46 C. Zhou, G. Y. Hao, P. Thomas, J. B. Liu, M. X. Yu, S. S. Sun, OK. Öz, X. K. Sun and J. Zheng, *Angew. Chem. Int. Ed.*, 2012, 51, 10118-10122

47 C. Jones and D. W. Grainger, *Adv. Drug Deliv. Rev.*, 2009, 61, 438-456.

Figure captions:

Scheme 1 Schematic illustration of the strategy for analysis of trypsin. Photographs of solutions illuminated with UV light (365 nm) illustrate the fluorescence of GSH-CdTe QDs under the

different conditions of the assay.

Fig. 1 (A) (a) UV−vis absorption spectrum and (b) fluorescence emission spectrum (λex= 380 nm) of the GSH-CdTe QDs; Inset: Photograph under UV light (365 nm) of the GSH-CdTe QDs. (B) TEM image of GSH-CdTe QDs.

Fig. 2 The pH effect on (a) the QDs quenched fluorescence efficiency by 140 nM cyt.c and (b) the QDs recovered fluorescence efficiency in the presence of 187.5 nM trypsin in the 50 mM Tris-HCl buffer at pH 6.5, 7, 7.5, 8, 8.5, 9, 9.5.

Fig. 3 (A) Fluorescence emission spectra of the QDs-cyt.c complex in the presence of increasing trypsin concentrations (0-375 nM). (a) QDs, (b) the QDs-cyt.c complex, (c) the QDs-cyt.c complex incubation with 375 nM trypsin. Inset: Photograph under UV light. (B) The relative fluorescence intensity of QDs-cyt.c complex after 15 min of incubation with (1) trypsin, (2) ALP, (3) lysozyme, (4) thrombin, (5) glucose oxidase, (6) pepsin, (7) lipase, (8) α-amylase, (9) BSA, (10) proline, (11) glycine, (12) tyrosine, (13) cysteine, (14) glutamic acid, (15) aspartic acid, (16) methionine and (17) no analyte at 37 ℃. The concentrations of trypsin and ALP were 375 nM and 3 unit mL^{-1}, respectively. The concentrations of (3), (4), (5), (6), (7), (8) and (9) were all 30 μg mL^{-1}. The concentrations of (10), (11), (12), (13), (14), (15) and (16) are all 0.5 mM. F_0 and F are the fluorescence intensity of QDs-cyt.c complex in the absence and presence of trypsin and the other analytes, respectively. The error bars represent the standard deviation of three measurements. Solution conditions: the complex of QDs (53.4 nM) and cyt.c (140 nM) was incubated with analytes in 50 mM Tris-HCl buffer at pH 8.5.

Fig. 4 (A) Fluorescence intensity changes of the QDs-cyt.c complex against time after addition of trypsin. (B) Dependence of initial rate of reaction (v_0) on trypsin concentration [trypsin]. (C) Dependence of kinetic parameters (V_{max}/K_m) on trypsin concentration. The error bars represent the standard deviation of three measurements. Solution conditions: the complex of QDs (53.4 nM) and cyt.c (140 nM) was incubated with various trypsin concentrations in 50 mM Tris-HCl buffer (pH 8.5) at 37 ℃.

Fig. 5 (A) Fluorescence intensity changes of the QDs-cyt.c complex as a function of the trypsin digestion time with different amounts of inhibitor. (B) Dependence of initial rate of reaction (v_0')

on BBI concentration. (C) Plot of the inhibition efficiency of BBI toward trypsin versus the concentration of BBI. The error bars represent the standard deviation of three measurements. Solution conditions: the solution of QDs (53.4 nM), cyt.c (140 nM) and trypsin (125 nM) was incubated with various BBI concentrations in 50 mM Tris-HCl buffer (pH 8.5) at 37 ℃.

Fig. 6 Fluorescence microscopic images of living PANC-1 cells: (A) cells incubated with the QDs-cyt.c for 30 min at 37 ℃, (B, C) cells were pretreated with BBI (1.25, 2.5 μg mL-1) for 15 min at 37 ℃ separately, then were incubated with the QDs-cyt.c for 30 min at 37 ℃, (D, E, F) bright field image of living PANC-1 cells shown in panels (A, B, C). Original magnification was 200×.

Table 1   Results of trypsin determination in normal adult human serum.

Table 2   Results of trypsin determination in acute pancreatitis adult human serum.

Table of Contents

Label-free and real-time monitoring of trypsin activity in living cells by quantum-dot-based fluorescent sensors

Wenzhu Zhang,[a] Ping Zhang,[a] Shengzhou Zhang*[b] and Changqing Zhu*[a]
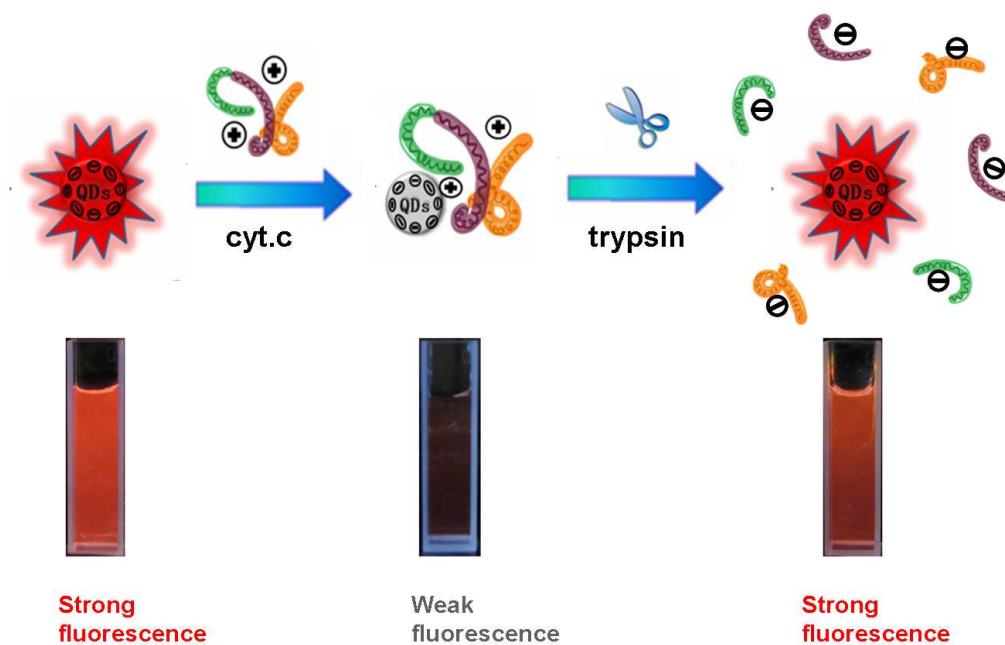
Description：

A quantum-dot-based fluoresence turn-on sensor was used for label-free and real-time monitoring of trypsin activity
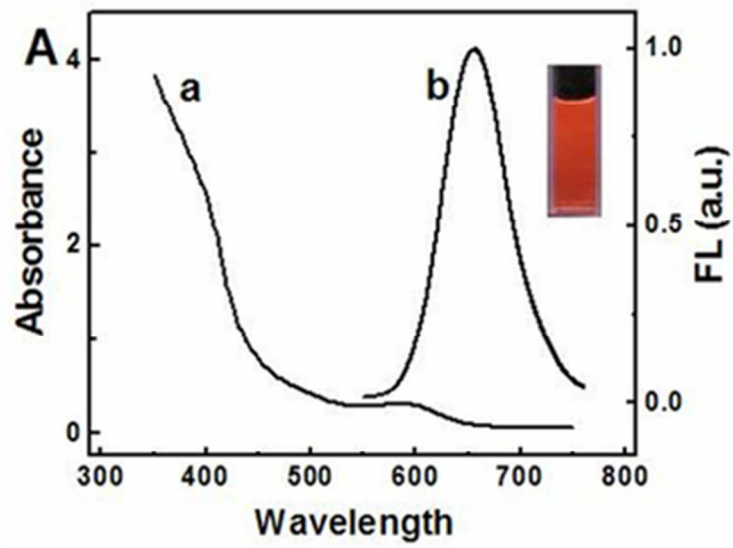
32x24mm (300 x 300 DPI)
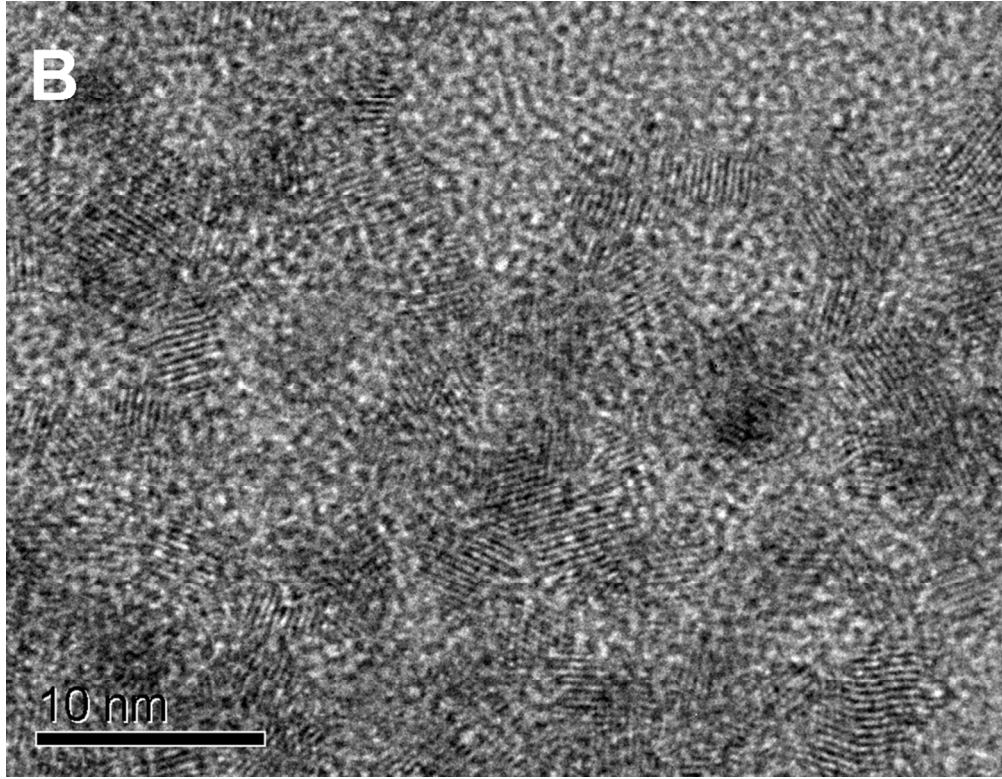
199x154mm (150 x 150 DPI)
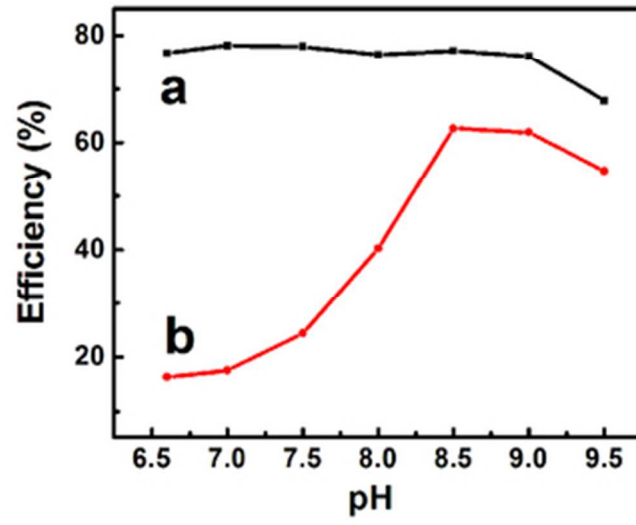
32x25mm (300 x 300 DPI)
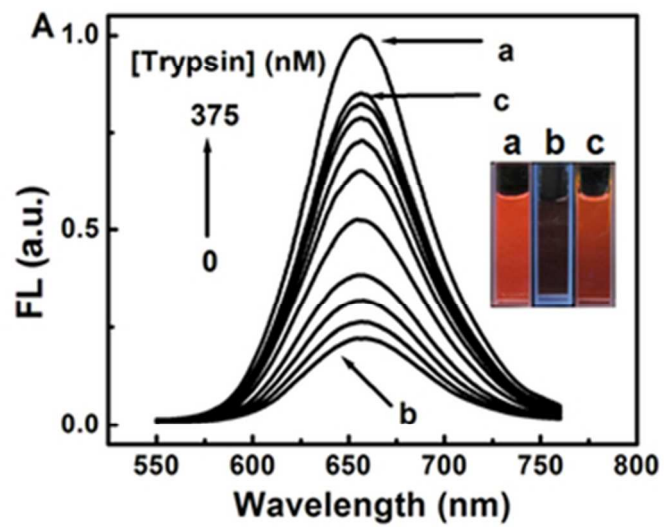
32x25mm (300 x 300 DPI)
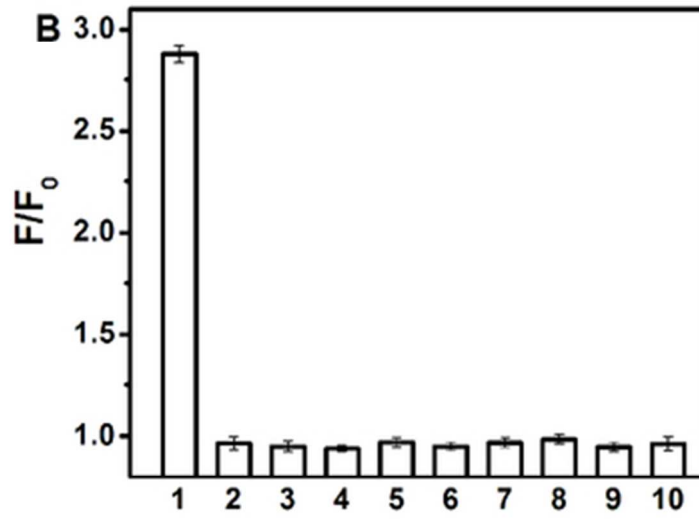
17x13mm (600 x 600 DPI)
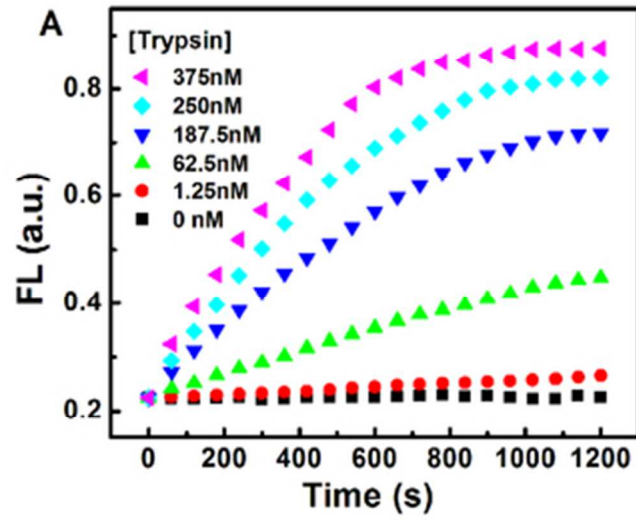
32x25mm (300 x 300 DPI)
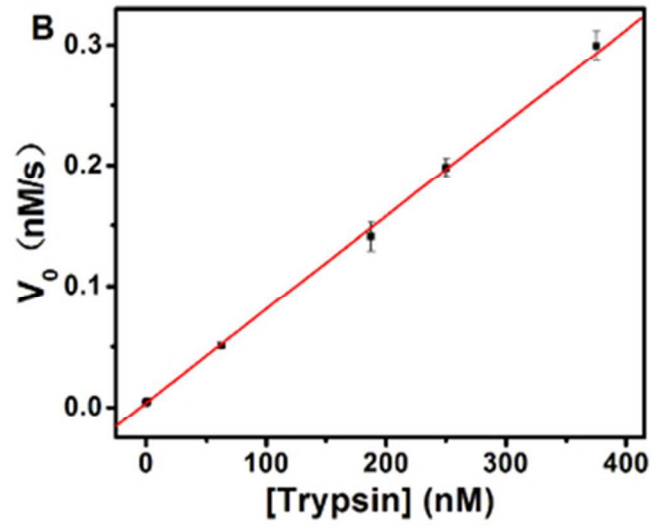
32x25mm (300 x 300 DPI)
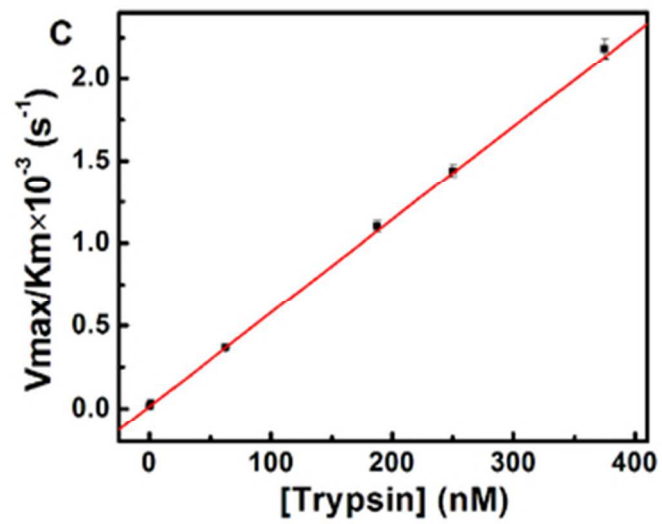
32x25mm (300 x 300 DPI)
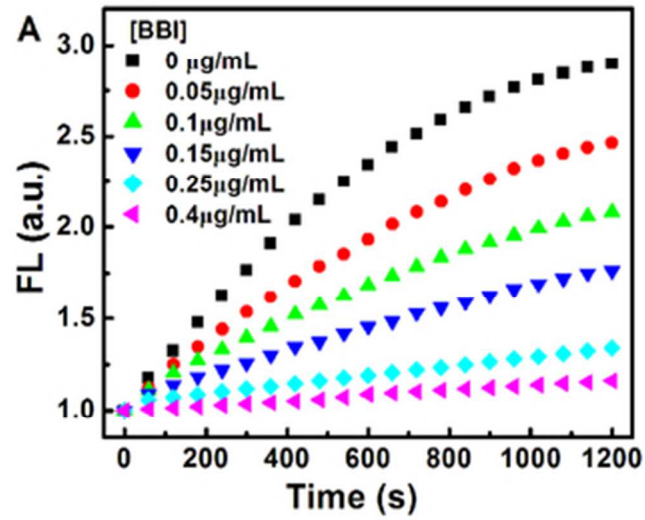
32x25mm (300 x 300 DPI)
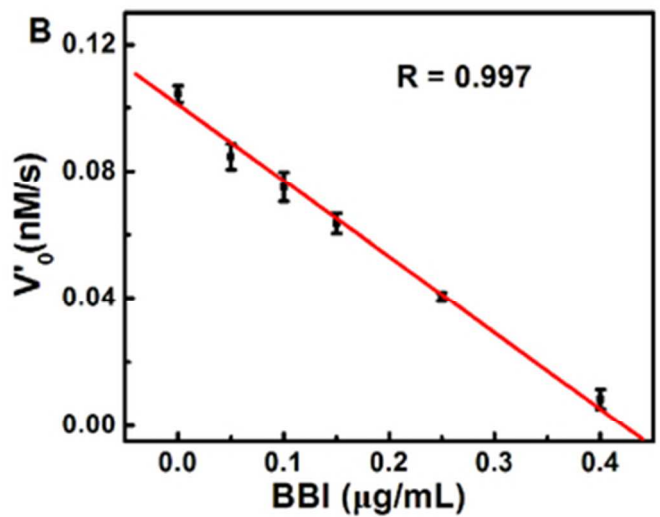
32x25mm (300 x 300 DPI)
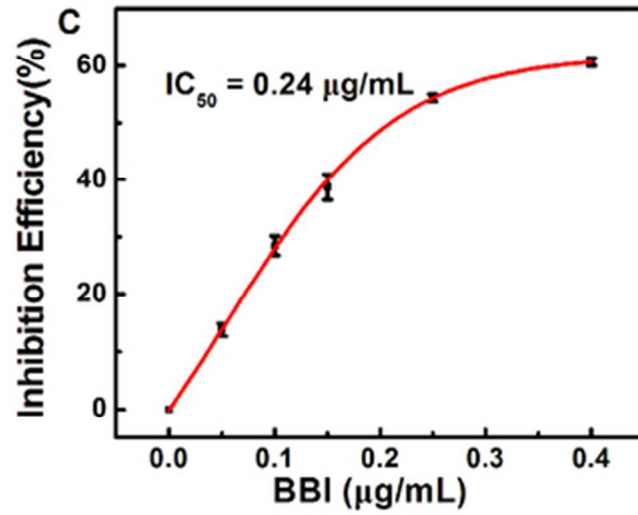
32x25mm (300 x 300 DPI)
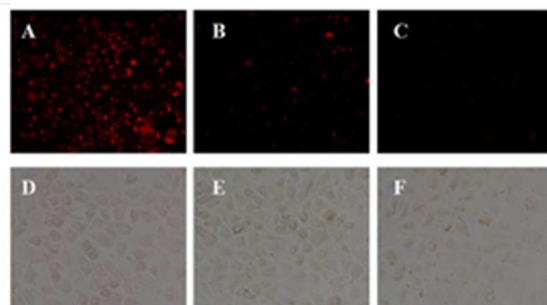
23x13mm (300 x 300 DPI)
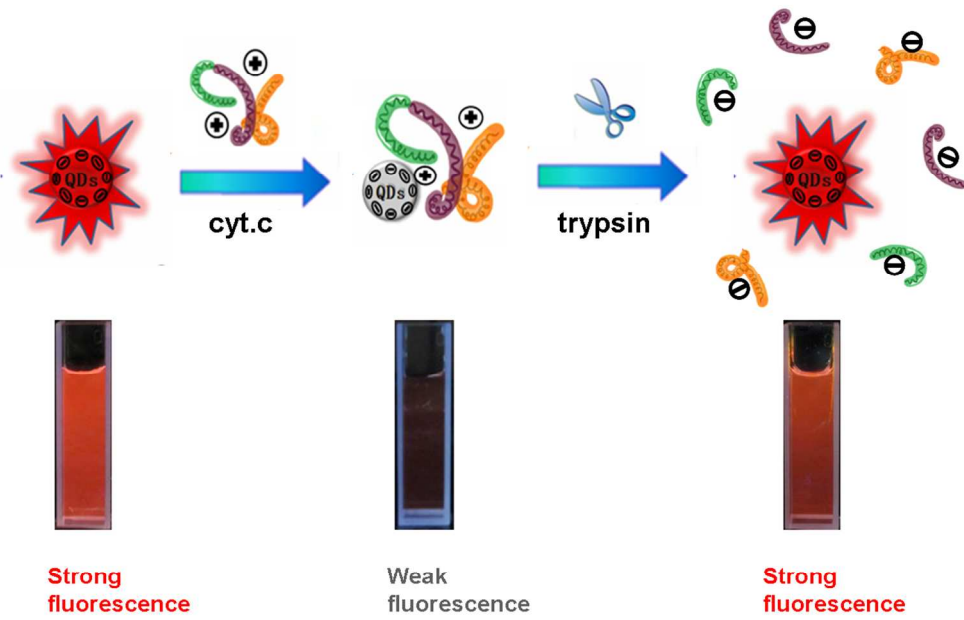
228x159mm (150 x 150 DPI)

Table 1   Results of trypsin determination in normal adult human serum

Samples	Measured[a]/ $\mu g\ mL^{-1}$	Trypsin added/ $\mu g\ mL^{-1}$	Recovered[a]/ $\mu g\ mL^{-1}$	RSD (%, n=6)	Recovery (%)
1	0.23	0.90	1.15	3.4	102.2
2	0.29	0.90	1.22	4.1	103.3
3	0.30	0.90	1.18	2.8	97.8

[a] Mean value of six determinations by the proposed method.

303x73mm (96 x 96 DPI)

Table 2   Results of trypsin determination in acute pancreatitis adult human serum

Samples	Measured[a]/μg mL^{-1}	BBI added /μg mL^{-1}	Recovered[a]/μg mL^{-1}	RSD (%, n=6)
1	1.71	0.10	0.64	3.4
2	1.84	0.10	0.76	3.9
3	1.93	0.10	0.88	2.2

[a] Mean value of six determinations by the proposed method.

303x65mm (96 x 96 DPI)